euspen's 21st International Conference & Exhibition, Copenhagen, DK, June 2021
www.euspen.eu

Load cell with adjustable stiffness based on a preloaded T-shaped flexure pivot

Loïc Tissot-Daguette[1], Michal Smreczak[1], Charles Baur[1] and Simon Henein[1]

[1]*Instant-Lab, EPFL, Switzerland*

loic.tissot-daguette@epfl.ch

Abstract

In this paper, we present a new flexure-based load cell with adjustable stiffness designed for force sensors with extended force range and respective measuring resolution. This novel monolithic mechanism consists of a T-shaped flexure pivot combined with an adjustable elastic preloading element. In particular, the compression preload can be adjusted to reach near-zero stiffness, i.e., very high sensor sensitivity, or to reach negative stiffness, i.e., a bistable behavior leading to a passive force-limiting device. The analytical model based on Euler-Bernoulli beam theory is derived in order to extract a non-linear formula of the pivot stiffness as a function of its preload. The results of finite element simulations carried out to verify the analytical model are presented. Based on these models, a mesoscale load cell has been dimensioned aiming for a force resolution of 50 nN when tuned to near-zero positive stiffness, approaching that of micro-force sensing nanoprobes.

Force sensor, Load cell, Compliant mechanism, Zero stiffness, Bistable mechanism, Beam buckling

1. Introduction

Over the past decades, the number of applications requiring precise measurement of forces down to the nanonewton range has rapidly increased. At microscale, beyond human perception, force sensing is important for assessing interactions with objects [1]. Examples of micromanipulation in which the measurement of such forces is beneficial are: electrical nanoprobing [2], biology [3] and microassembly [4].

Load cells are transducers converting forces into electrical signals. A common type of load cells is based on compliant mechanisms where a part of the mechanism deflects proportionally to the applied force, following Hooke's law, which presents a number of advantages [5]. Nanonewton resolution load cells are found in microelectromechanical systems (MEMS) such as Atomic Force Microscope (AFM) cantilever-based probes dedicated to micromanipulation [6]. Various methods for adjusting the stiffness are known [7], which allow the precision of the force measurement to be adapted to specific applications. However, a probe integrated within the MEMS is an important disadvantage in case of multi-scaled applications (e.g., when switching from nano- to microprobe is required) or if the probe needle gets damaged or contaminated.

Currently, there is no load cell on the market dedicated to micromanipulation that offers stiffness adjustment capabilities along with the possibility to replace the probe. The contributions of this paper are the following: (i) a novel mesoscale compliant load cell with adjustable sensitivity and exchangeable probe is described, analyzed and dimensioned (Sec. 2); (ii) the design approach is validated by FEM simulations (Sec. 3); and (iii) the mechanical behavior and fabrication limits are discussed (Sec. 4) in order to manufacture and test a load cell in forthcoming work.

2. Design of a load cell with a tunable stiffness

2.1. Mechanism description

The new load cell mechanism proposed in this paper, called TIVOT, is a 1-DOF flexure rotative joint with tunable angular stiffness (patent pending). Its schematic is shown in Fig. 1. In this design, a flexure pivot is made of three identical blades arranged in a T-shaped structure, with two blades attached to the fixed frame and one blade linked to a preload mechanism. The preload mechanism exerts a compressive force to the two horizontal blades of the pivot in order to decrease their bending stiffness and thus the overall pivot angular stiffness K_α. This preload is achieved by the deformation of a linear spring with constant stiffness K_0 and controlled by the displacement x_0 of a linear stage (schematically actuated by a screw in Fig. 1). When the pivot is rotated, a displacement x_p of the passive linear stage is induced due to the end-shortening of the horizontal blades.

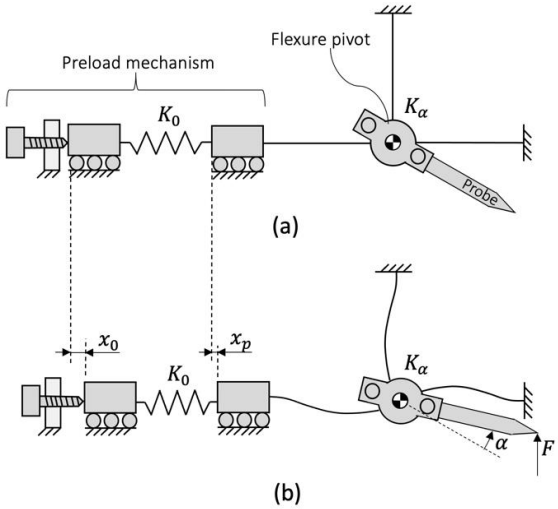

Figure 1. (a) TIVOT at rest (i.e., no energy is stored in the mechanism). (b) TIVOT preloaded and a force applied at the probe tip.

Using a probe mounted on the flexure pivot, a force F can be measured when applied at the probe tip creating a moment on the pivot. Based on the pivot stiffness K_α (controlled by the preload displacement x_0), the probe rotates by an angle α which can be measured using a displacement sensor. The load cell can

be monolithic if the linear stages and the spring are realized with flexures. The center of mass of the probe must be coincident with the center of rotation of the pivot to reduce gravity effects on the mechanism behavior. The main benefit of the TIVOT is that tuning the stiffness of the pivot allows to adjust the load cell sensitivity thus permitting to adapt the force range and respective resolution. Nanonewton forces can be sensed if the flexure pivot is well-adjusted to near-zero positive stiffness. The results in Sec. 3 show that negative stiffness can also be achieved with high preloads, leading to a bistable mechanism.

2.2. Analytical model

This section introduces the theoretical model used to design the TIVOT mechanism. For the calculations, we assume that the three blades of the pivot are initially straight slender beams and the two horizontal blades have the same deflected shape. Thereby, we will consider the rotation stiffness of a single blade compressed by a preload P and compute its horizontal displacement, to then evaluate the stiffness of the whole TIVOT mechanism and the pivot moment-angle relation.

Figure 2 shows the deformation and the load case of one of the beams. The beam is clamped at one end and hinged with a rigid lever of length p at the other extremity. The horizontal displacement Δx of the pivot is considered and its vertical displacement is neglected for simplification purposes. A torque $M_{\alpha,1\text{beam}}$ (created by the force at the probe tip in Fig. 1) is applied to the pivot which rotates by an angle α. The free-body diagram of the beam is derived in order to compute the pivot stiffness as a function of the compressive preload P.

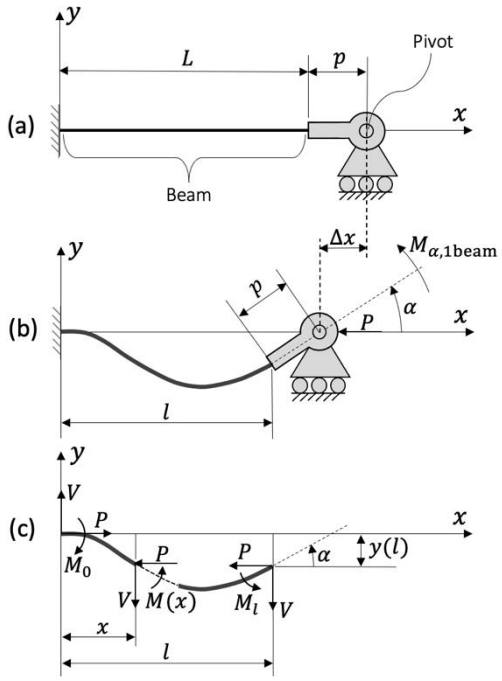

Figure 2. (a) As-fabricated, (b) deformed and (c) free-body diagram of one of the TIVOT beams.

Considering small beam deformations, we compute the blade deflection using Euler-Bernoulli static beam equation:

$$M(x) = EIy''(x) \tag{1}$$

where EI is the beam flexural rigidity and $M(x)$ is the bending moment related to the beam reaction forces and moment:

$$M(x) = -Py(x) + Vx + M_0 \tag{2}$$

Combining Eqs. (1) and (2) gives a second-order differential equation. After deriving the general solution and integrating the boundary conditions $y(0) = y'(0) = 0$, we obtain the beam deflection:

$$y(x) = A(\sin(kx) - kx) + B(\cos(kx) - 1) \tag{3}$$

where:

$$k = \sqrt{\frac{P}{EI}} \tag{4}$$

The parameters A and B are found using the boundary conditions $y(l) \cong -p\alpha$ and $y'(l) \cong \alpha$:

$$A = -\alpha l \frac{\cos(kl) - 1 - kl\,\bar{p}\sin(kl)}{kl\big(kl\sin(kl) + 2(\cos(kl) - 1)\big)} \tag{5}$$

$$B = -\alpha l \frac{kl - \sin(kl) - kl\,\bar{p}(\cos(kl) - 1)}{kl\big(kl\sin(kl) + 2(\cos(kl) - 1)\big)} \tag{6}$$

where:

$$\bar{p} = \frac{p}{l} \tag{7}$$

We define the rotation stiffness of a single beam as follows:

$$K_{\alpha,1\text{beam}} = \frac{M_{\alpha,1\text{beam}}}{\alpha} \cong \frac{M_l + Vp + Py(l)}{y'(l)} = \frac{EI}{l} kl \frac{kl\cos(kl) - \sin(kl)\,(1 + (kl)^2\bar{p} + (kl)^2\bar{p}^2)}{kl\sin(kl) + 2(\cos(kl) - 1)} \tag{8}$$

The horizontal displacement Δx comes from the rotation of the lever and the end-shortening of the beam. In order to calculate this displacement, as in [8] we use the approximation:

$$\Delta x = L - l + p(1 - \cos(\alpha)) \cong \int_0^l \frac{\big(y'(x)\big)^2}{2} dx + \frac{p\alpha^2}{2} = H(kl)\alpha^2 \tag{9}$$

where:

$$H(kl) = \frac{kl}{8l}\left[\left(\frac{A}{\alpha}\right)^2 (6kl - 8\sin(kl) + \sin(2kl)) + 2\left(\frac{A}{\alpha}\right)\left(\frac{B}{\alpha}\right)(\cos(2kl) - 4\cos(kl) + 3) + \left(\frac{B}{\alpha}\right)^2 (2kl - \sin(2kl))\right] + \frac{p}{2} \tag{10}$$

The TIVOT flexure pivot stiffness K_α is the sum of the three beam stiffnesses (see Fig. 1). Because the two horizontal blades are preloaded by the compressive force P, and the vertical blade is not preloaded (i.e., from Eq. (4), $kl = 0$), it leads to:

$$K_\alpha = 2K_{\alpha,1\text{beam}} + K_{\alpha,1\text{beam}}(kl = 0) = 2K_{\alpha,1\text{beam}} + \frac{4EI}{l}(1 + 3\bar{p} + 3\bar{p}^2) \tag{11}$$

To obtain the TIVOT nonlinear moment-angle behavior (M_α as a function of α), we need to consider the variation of the load P due to the horizontal displacement x_p (x_0 being fixed). First, the force P is linked to the linear spring deformation with the following relation:

$$P = K_0(x_0 - x_p) \tag{12}$$

where the displacement x_p is assumed to be the sum of the two horizontal beam displacements Δx derived in Eq. (9):

$$x_p = 2\Delta x = 2H(kl)\alpha^2 \tag{13}$$

Using Eqs. (4), (12) and (13), we can obtain the pivot angle α:

$$\alpha = \pm\sqrt{\frac{x_0 - \frac{EI}{K_0 l^2}(kl)^2}{2H(kl)}} \quad (14)$$

Hence, from Eqs. (11) and (14), the applied moment can finally be calculated as:

$$M_\alpha = K_\alpha \alpha \quad (15)$$

2.3. Proposed dimensions

Using the analytical model in the previous section, a flexure-based mesoscale embodiment of the TIVOT (see Fig. 3 and Table 1) was designed to demonstrate that the stiffness tuning works as expected, to provide numerical results for comparison to the theoretical model and discuss possible manufacturing limits.

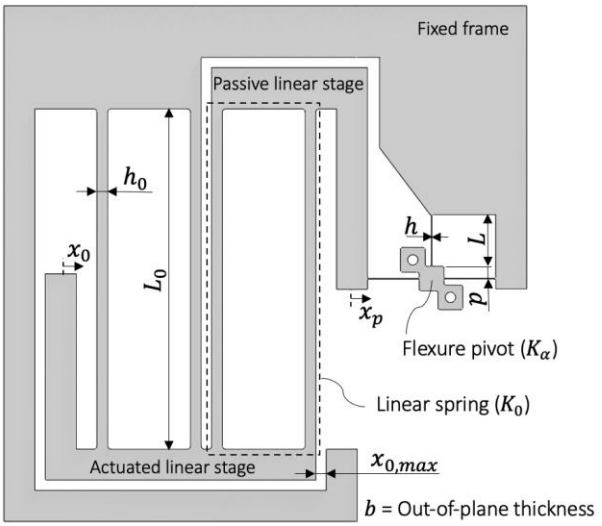

Figure 3. Mesoscale load cell prototype (illustrated as-fabricated). Two holes are drilled in order to mount a probe on the flexure pivot.

To make the mechanism structurally monolithic, the linear stages and the linear spring are replaced by two identical parallel spring stages. The stiffness of each parallel spring stage is given by $K_0 = 2Eb_0h_0^3/L_0^3$ [5].

Table 1. Design parameters of the load cell.

	Parameter	Value
Material (Ti-Al6-V4)	E	114 GPa
	σ_y	830 MPa
Flexure pivot	h	80 µm
	b	2 mm
	L	4.5 mm
	p	1.4 mm
	α_{max}	5 deg
Preload mechanism	h_0	1.05 mm
	b_0	2 mm
	L_0	33 mm
	K_0	14.7 N/mm
	$x_{0,max}$	1 mm

The material of the load cell structure is chosen to be titanium (Ti-Al6-V4), well suited for its high yield strength on Young's modulus ratio (σ_y/E). The structure is designed to be manufactured with wire-cut electrical discharge machining (EDM) process, allowing cutting blades with thicknesses down to 50 µm and machining tolerances of a few µm. In terms of load cell requirements, we aim for a maximum pivot stiffness (when non-preloaded) lower than 60 Nmm/rad.

3. FEM results

To validate our designed load cell, a finite element method (FEM) static study was carried out using Comsol Multiphysics 5.4 considering geometric nonlinearities (for analyzing prestressed structures). A first study was conducted to validate that the material sustains the internal stress when the load cell structure is maximally deformed ($\alpha = 5$ deg and $x_0 = 1$ mm). Figure 4 shows that the maximum von Mises stress in the structure is 696 MPa which is below the material yield stress stated in Table 1.

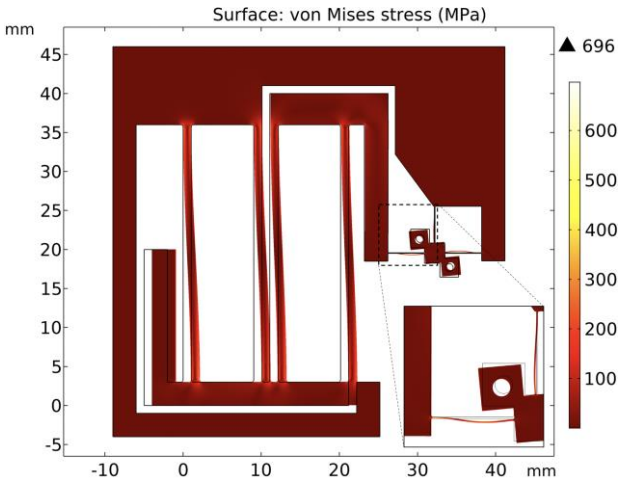

Figure 4. FEM simulation of the load cell structure.

Figure 5 illustrates the simulated pivot stiffness-preload graph for small pivot angles ($\alpha \cong 0$). The simulation results of the pivot moment-angle relation for different preloading displacements are shown in Fig. 6. From Eqs. (11), (14) and (15) of Sec. 2.2, analytical curves are traced out in Figs. 5 and 6 as the parameter kl ranges from 0 (no preload) to 2π (Euler's critical load of a clamped-clamped beam [9]), with the design parameters stated in Table 1 and the approximation $l \cong L$. We avoid $kl \geq 2\pi$ because the horizontal beams start to buckle even if the pivot angle α is maintained to zero. This elastic instability leads to hysteresis in the moment-angle curve and the stress in the structure rises sharply due to the large beam deformations.

Table 2 indicates the theoretical force sensitivity, resolution and range of the load cell that should be obtained on a test bench containing a probe needle mounted on the load cell with a length (distance from pivot center of rotation to probe tip) of 25 mm and a laser proximity sensor with a resolution of 10 nm (for the conversion of the load cell deflection into an electrical signal) measuring the displacement at the probe tip. The force range is considered here to be the maximum theoretical measured force when the pivot angle stroke is mechanically stopped at 5 deg.

Table 2. Theoretical force sensitivity, resolution and range of the load cell for: 1) non-preloaded pivot and 2) near-zero positive stiffness pivot.

Pivot stiffness tuning	x_0 [mm]	Sensitivity [m/N]	Resolution [µN]	Range [mN]
1) Non-preloaded	0	0.01	1	200
2) Near-zero positive stiffness	0.6	0.2	0.05	20

4. Discussion

4.1. Stiffness tuning

It is observed that the FEM predicts similar results as compared with the analytical model. In Fig. 5, both simulation and theoretical results show that the preload allows to tune the load cell stiffness. Three stiffness regions stand out: *positive stiffness*; *negative stiffness; and hysteretic stiffness.*

Positive stiffness corresponds to the primary use of the load cell for force sensing applications. As shown in Table 2, the force resolution can be adjusted from 1 µN down to 50 nN. If well-tuned the resolution could decrease even more. However, the lower the resolution, the lower the measuring range. Hence, we should adjust the preloading according to the range of forces we need to measure. We can add that load cell stiffnesses could be higher than the non-preloaded pivot stiffness if the preload mechanism applies a tensile preload (instead of a compressive preload) to the pivot. Even if it is not presented in the results, the analytical model in Sec. 2.2 can consider tensile preloads if the parameter k (defined in Eq. (4)) is a complex number.

Negative stiffness is reached when exceeding the zero stiffness pivot preload (see Fig. 5). This bistable behavior could open a broader range of applications, such as, but not limited to, force threshold sensors, force limiting devices, non-volatile bistable mechanical memories or constant-force mechanisms if combined with a preloaded positive-stiffness mechanism in parallel.

We call the region *hysteretic stiffness* when the preloading displacement is higher than 1.3 mm, because there exist multiple pivot stiffness solutions for the same pivot angle. Indeed, the moment-angle characteristics of the pivot depends on the current buckling direction of the horizontal beams. This hysteresis aspects of the TIVOT could be further investigated in future studies using the analytical model presented in this paper.

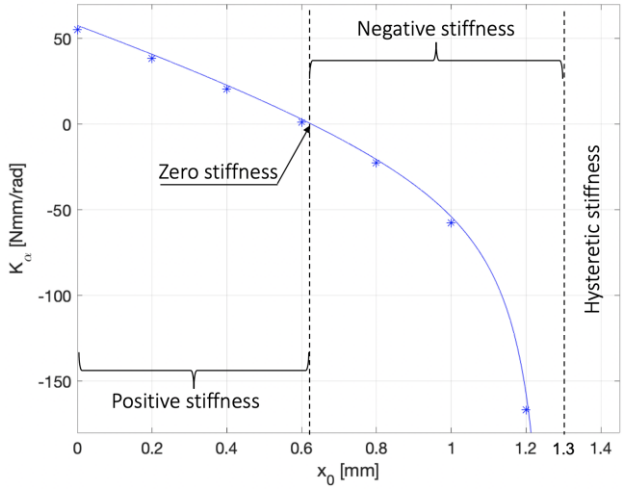

Figure 5. Angular stiffness versus axial preload of the TIVOT for small pivot angles ($\alpha \cong 0$). Theoretical results are represented by a solid line and the FEM numerical results are represented by stars.

4.2. Load cell nonlinearities

In Fig. 6, both simulation and theoretical results show nonlinearity. We can also notice that the numerical moment-angle characteristics is asymmetrical with respect to the angle direction compared to the theoretical curve. The discrepancy between the analytical and FEM results is considered to be primarily due to the neglection of the pivot vertical displacement in the analytical model. The stiffness nonlinearities of the TIVOT could be compensated using a dedicated circuit hardware to linearize the electrical output of the displacement sensor or using linearization algorithms in a controller/processor embedded or not in the force sensor.

4.3. Manufacturing limits

Gravity can affect the measured force if the center of mass of the probe is not coincident with the center of rotation of the pivot. To precisely compensate the imbalance of the probe, we can use e.g., an adjustable constant torque mechanism mounted in parallel on the load cell pivot. Depending on the load cell environment, the force sensitivity can fluctuate due to temperature variations. Instead of EDM fabricated metal structure, we could use materials with low thermal sensitivity such as glass (using femtolaser 3D printing technology) or oxidized silicon (using deep reactive ion etching process).

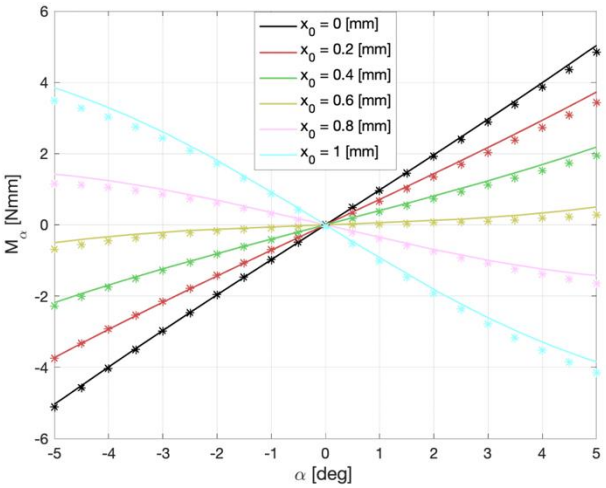

Figure 6. Moment-angle characteristics of the TIVOT for different preload displacements. Theoretical results are represented by solid lines and the FEM numerical results are represented by stars.

5. Conclusion

A novel flexure-based load cell with tunable stiffness is presented in this paper. Analytical modeling is conducted based on Euler-Bernoulli beam theory and verified by carrying out FEM simulations. Based on these models, a monolithic mesoscale load cell is designed. The results show that the load cell force resolution can be adjusted from 1 µN down to 50 nN with a measuring force range of 200 mN and 20 mN respectively. Interestingly, the mechanism becomes bistable for certain adjustments, leading to a broader range of applications (force limiting devices, force threshold sensors, etc.).

Future work includes a verification of the analytical and numerical solutions by experimental results from a load cell prototype fabricated in titanium using wire-cut EDM process.

References

[1] Bolopion A and Régnier S, 2013, A review of haptic feedback teleoperation systems for micromanipulation and microassembly, *IEEE Transactions on Automation Science and Engineering*, **10(3)**, 496–502

[2] Ma Z and Seiler D G (Eds.), 2016, *Metrology and Diagnostic Techniques for Nanoelectronics*, 1317-39

[3] Xu Q, 2018, *Micromachines for Biological Micromanipulation*, Springer International Publishing, 1-13

[4] Rabenorosoa K, Clévy C and Lutz P, 2010, Active force control for robotic micro-assembly: Application to guiding tasks, *2010 IEEE International Conference on Robotics and Automation*, Anchorage, AK, 2137-42

[5] Cosandier F, Henein S, Richard M and Rubbert L, 2017, *The Art of Flexure Mechanism Design*, EPFL Press, Lausanne

[6] Kim D H, Kim B and Park J O, 2004, Implementation of a Piezoresistive MEMS Cantilever for Nanoscale Force Measurement in Micro/Nano Robotic Applications, *KSME International Journal*, **18(5)**, 789–797

[7] De Laat M L C, Pérez Garza H H, Herder J L and Ghatkesar M K, 2016, A review on in situ stiffness adjustment methods in MEMS, *Journal of Micromechanics and Microengineering*, **26(6)**

[8] Vangbo M, 1998, An analytical analysis of a compressed bistable buckled beam, *Sensors and Actuators*, *A* **69**, 212-216

[9] Chajes A, 1974, *Principles of Structural Stability Theory*, Prentice-Hall, Englewood Cliffs, NJ, 8-10